Chromatic dispersion measurement of holey fibres using a supercontinuum source and a dispersion balanced interferometer

P. Hlubina [a,*] , M. Kadulová [a], P. Mergo [b]

[a] *Department of Physics, Technical University Ostrava, 17. listopadu 15, 708 33 Ostrava-Poruba, Czech Republic*

[b] *Laboratory of Optical Fibre Technology, Maria Curie-Sklodowska University, Pl. M. Curie-Sklodowskiej 3, 20-031 Lublin, Poland*

Abstract

Chromatic dispersion of polarization modes in short-length holey fibres is measured by a spectral interferometric technique employing a broad-band supercontinuum source. The technique utilizes a dispersion balanced Mach-Zehnder interferometer with a fibre under test of known length inserted in one of the interferometer arms and the other arm with adjustable path length. We record a series of spectral interferograms to measure the equalization wavelength as a function of the path length difference, or equivalently the differential group index dispersion of the fibre. A five-term power series fit is applied to the measured data to obtain the chromatic dispersion over a broad spectral range (500–1600 nm). We measured by this technique the chromatic dispersion of polarization modes in four air-silica holey fibres and revealed the dependence of the position of the zero-dispersion wavelength on the geometrical parameters of the fibre.

Key words: spectral interferometry, supercontinuum source, Mach-Zehnder interferometer, birefringent fibre, chromatic dispersion, zero-dispersion wavelength
PACS: 07.60, 42.25.Hz, 42.81.Cn

* Tel.: +420-597-323-134; fax: +420-597-323-139.
Email address: petr.hlubina@vsb.cz (P. Hlubina).

Preprint submitted to Elsevier Science *19 November 2012*

1 Introduction

The group index dispersion of optical fibres measured precisely over a broad spectral range is an important characteristic playing a crucial role in research areas such as high-speed optical transmission systems, broadband optical communications and supercontinuum generation. The chromatic dispersion, which can be obtained by simply differentiating the group index, is a significant characteristic that affects the bandwidth of a high-speed optical transmission system through pulse broadening and nonlinear optical distortion. Chromatic dispersion of long-length optical fibres is determined by two widely used methods [1]: the time-of-flight method, which measures relative temporal delays for pulses at different wavelengths, and the modulation phase shift technique [2], which measures the phase delay of a modulated signal as a function of wavelength.

White-light interferometry employing a broadband source in combination with a standard Michelson or a Mach-Zehnder interferometer [3] is considered as one of the best tools for dispersion characterization of short-length optical fibres. White-light interferometry usually utilizes a temporal method [4] or a spectral method [5–13]. The spectral method is based on the observation of spectral fringes in the vicinity of a stationary-phase point [5–12] or far from it [13]. Recently, a virtual reference spectral interferometric technique for measuring chromatic dispersion of short-length fibres has been presented [14].

The feasibility of the interferometric techniques has been demonstrated in measuring the dispersion of holey fibres (HFs) [15,16]. One of the most successful applications of HFs, employing high effective nonlinearities and an excellent control of chromatic dispersion with the zero-dispersion wavelength (ZDW) at the operating wavelength of widely available mode-locked Ti:sapphire lasers, is supercontinuum generation [17]. Endlessly single-mode [18] and highly-birefringent [19,20] HFs for supercontinuum generation have also been designed and fabricated with the ZDW close to a 1064 nm of a microchip laser, enabling savings in size and cost. Moreover, a supercontinuum source has enabled dispersion measurement over a broad spectral range [16].

The aim of this paper is to present a substantially improved spectral-domain interferometric technique, which allows us to measure chromatic dispersion of pure silica highly birefringent HFs over a broad spectral range (500–1600 nm), including a precise determination of the ZDW. The technique employs a broad-band supercontinuum source and a dispersion balanced Mach-Zehnder interferometer (MZI). There is no need to calibrate the dispersion in the reference arm of the MZI so that this technique is more accurate in comparison with that demonstrated in our previous paper [11]. Moreover, the supercontinuum source substituting a halogen lamp used in our previous experiments [9,11,12]

allows for a broad spectral range and less time consuming measurement of the chromatic dispersion.

2 Experimental Method

Consider a dispersion balanced MZI as shown in Fig. 1 with a birefringent fibre under test (FUT) of length z that supports two polarization modes over a broad spectral range. The birefringent FUT with the effective phase indices $n_x(\lambda)$ and $n_y(\lambda)$ is placed in the first (test) arm of the interferometer and the other (reference) arm is with the adjustable path length L in the air. Next, consider that the transmission azimuth of both the polarizer and the analyzer is aligned parallel to the shorter polarization axis of the FUT, i.e., only the y-polarization mode is guided by the FUT and its dispersion is measured in the set-up. The group optical path difference (OPD) $\Delta^{\mathrm{g}}_{\mathrm{MZ}}(\lambda)$ between the beams in the MZI is given by

$$\Delta^{\mathrm{g}}_{\mathrm{MZI}}(\lambda) = L - l - N_y(\lambda)z, \tag{1}$$

where l is the path length in the air in the test arm of the MZI and $N_y(\lambda)$ is the group effective index of the y-polarization mode of the FUT, defined as

$$N_y(\lambda) = n_y(\lambda) - \lambda\frac{\mathrm{d}n_y(\lambda)}{\mathrm{d}\lambda}. \tag{2}$$

After recombining the beams at the output of the MZI, the spectral interference fringes with the wavelength-dependent period are resolved. The interference fringes of the largest period are located in the vicinity of a stationary-phase point, satisfying the condition $\Delta^{\mathrm{g}}_{\mathrm{MZ}}(\lambda_0) = 0$ at the equalization wavelength λ_0 [22]. This means that for the path length $L = L(\lambda_0)$ we obtain from Eq. (1)

$$L(\lambda_0) = N_y(\lambda_0)z + l. \tag{3}$$

If one of the equalization wavelengths, λ_{0r}, is chosen as the reference one, the path length difference $\Delta L(\lambda_0)$ is given by

$$\Delta L(\lambda_0) = \Delta N_y(\lambda_0)z, \tag{4}$$

where $\Delta N_y(\lambda_0)$ is the differential group index defined as

$$\Delta N_y(\lambda_0) = N_y(\lambda_0) - N_y(\lambda_{0r}). \tag{5}$$

Therefore, measuring the path length difference $\Delta L(\lambda_0)$ as a function of the equalization wavelength λ_0 and using Eq. (4), the dispersion of the differential group index $\Delta N_y(\lambda_0)$ of the y-polarization mode can be determined.

The chromatic dispersion $D_y(\lambda)$ of the y-polarization mode of the FUT is given by

$$D_y(\lambda) = \frac{1}{c}\frac{\mathrm{d}[\Delta N_y(\lambda)]}{\mathrm{d}\lambda}, \tag{6}$$

where $\Delta N_y(\lambda)$ is a Laurent polynomial fit of the measured wavelength dependence of the differential group index $\Delta N_y(\lambda_0)$ and c is the free-space velocity of light.

Similarly, when the transmission azimuth of both the polarizer and the analyzer is aligned parallel to the longer polarization axis of the FUT, i.e., the x-polarization mode is guided by the FUT, the chromatic dispersion $D_x(\lambda)$ can be measured in the set-up. Eventually, the results of measurement of the group modal birefringence $G(\lambda) = N_x(\lambda) - N_y(\lambda)$ by a method of spectral-domain tandem interferometry [22] can be utilized.

Moreover, treating air-silica highly birefringent HFs, the measured group modal birefringence $G(\lambda)$ can be approximated as [21]

$$G(\lambda) = (1-m)\xi\lambda^m, \tag{7}$$

where ξ and m are constants. The chromatic-dispersion difference $D_p(\lambda)$, which is defined as

$$D_p(\lambda) = D_x(\lambda) - D_y(\lambda) = \frac{1}{c}\frac{\mathrm{d}[G(\lambda)]}{\mathrm{d}\lambda}, \tag{8}$$

can be approximated as

$$D_p(\lambda) = (1-m)m\xi\lambda^{m-1}/c. \tag{9}$$

The chromatic dispersion $D_x(\lambda)$ of the x-polarization mode is given as

$$D_x(\lambda) = D_p(\lambda) + D_y(\lambda). \tag{10}$$

Thus, from the chromatic-dispersion difference $D_p(\lambda)$ obtained from the measured group modal birefringence $G(\lambda)$ we can deduce the chromatic dispersion $D_x(\lambda)$ of the x-polarization mode in the FUT when the chromatic dispersion $D_y(\lambda)$ of the y-polarization mode is known.

3 Experimental set-up

The experimental set-up used to measure the chromatic dispersion of the y-polarization mode in FUT is shown in Fig. 1. Light emitted from supercontinuum source SCS (SC450-4, Fianium) with a splitter (Splitter-900, Fianium) and endlessly single-mode fibre ESMF (FDS-PCF, Fianium) passes through collimating lens C and enters a bulk-optic Mach-Zehnder interferometer with plate beam splitters BS1 and BS2 (BSW07, Thorlabs). The test arm of the interferometer comprises objective MO1 (10×/0.30, Meopta), the FUT and achromatic lens AL1 (74-ACR, Ocean Optics). The reference arm comprises a micropositioner connected to mirrors M3 and M4, microscope objective MO2 (10×/0.30, Meopta) and achromatic lens AL2 (74-ACR, Ocean Optics). The light from the output of the interferometer passes through aperture Ap and is focused by microscope objective MO3 (10×/0.30, Meopta) into the read fibre of a fibre-optic spectrometer (S2000 or NIR-512, Ocean Optics). The spectrometers S2000 and NIR-516 have a spectral operation range from 350 to 1000 nm and from 850 to 1700 nm, respectively.

The investigated HFs are pure silica highly birefringent fibres (labelled as FUT 1 to FUT 4) that were manufactured by a group from Maria Curie-Sklodowska University, Lublin, Poland. The geometrical parameters of measured HFs, including the cladding diameter Φ, pitch Λ, diameter d of small holes, diameter D of large holes (see Fig. 2) and length z, are listed in Table 1.

4 Experimental results and discussion

Prior to the measurements we used a laser diode instead of the supercontinuum source to check a precise alignment of the optical components and the proper excitation of the FUT: the elliptical-shape optical field at the output of the test arm indicated that the light was guided by the fibre core. The orientation of the analyzer was along the shorter axis of the elliptical core (see Fig. 2) so that the group dispersion of the y-polarization mode in the FUT was measured.

In the differential group index dispersion measurement of HF 2, the path length in the reference arm of the MZI was adjusted to resolve spectral interference fringes. Next, by displacement of mirrors M3 and M4 with a step of 10 or 50 μm, the path lengths in the MZI reference arm were adjusted, so that well separated and clean fringes on a sufficiently wide spectral range were observed. The width of the spectral interference fringes resolved for the length of HF2 was sufficient to determine the equalization wavelength λ_0 precisely. The spectral signals recorded by spectrometer S2000 revealed that the equaliza-

tion wavelength λ_0 can be resolved in the spectral range from 501 to 894 nm. Similarly, the spectral signals recorded by spectrometer NIR-516 revealed that the equalization wavelength λ_0 can be resolved in the spectral range from 916 to 1526 nm. The largest period of the interference fringes was observed in the vicinity of the equalization wavelengths, whose positions in the interference pattern changed in response to displacement of the mirrors. Figure 3 shows two examples of the spectral signals recorded for two different path length differences $\Delta L_1 = -640$ μm and $\Delta L_1 = -820$ μm adjusted in the MZI. The spectral signals clearly show the effect of the limiting resolving power of the spectrometers on the visibility of the spectral interference fringes in the vicinities of two different equalization wavelengths: 797.82 nm and 1403.31 nm for the spectral signal shown by the solid line; 943.67 nm and 1169.10 nm for the spectral signal shown by the dashed line. Two equalization wavelengths λ_{01} and λ_{02} are due to the minimum in the group index $N_y(\lambda)$ or in the differential group index $\Delta N_y(\lambda)$ located between the wavelengths λ_{01} and λ_{02}. The results of measuring the displacement as a function of the equalization wavelength, or equivalently the differential group index dispersion according to Eq. (4), are plotted in Fig. 4 by the crosses together with the solid line representing a five-term Laurent polynomial [11]

$$\Delta N_y(\lambda) = \frac{a_1}{\lambda^4} + \frac{a_2}{\lambda^2} + a_3 + a_4\lambda^2 + a_5\lambda^4. \tag{11}$$

Note that some experimental data are missed due to the superimposed interference fringes for which the equalization wavelengths cannot be resolved. Moreover, Fig. 4 shows that the differential group index dispersion is measured with a sufficiently large number of experimental data, illustrating the advantages of using a broad-band supercontinuum source versus a halogen lamp. Consequently, the broad-band spectral source allows for better fitting of the experimental data. The chromatic dispersion $D_y(\lambda)$, corresponding to the fit given by Eq. (11), is shown in Fig. 5 by the solid line. Measurement precision is better than 0.1 ps km^{-1}nm^{-1}.

In Fig. 6 are shown by crosses the measured values of the group modal birefringence $G(\lambda)$ that were obtained by a method of spectral-domain tandem interferometry [22]. A least-squares fit of $G(\lambda)$ according to Eq. (7) to the experimental data, which is shown in Fig. 6 by the solid line, gives $m = 2.274$ and $\xi = 3.957 \cdot 10^{-11}$. The chromatic-dispersion difference $D_p(\lambda)$, determined from Eq. (9), is shown in Fig. 6 by the dashed line. The chromatic-dispersion difference $D_p(\lambda)$ was also used to obtain the wavelength dependence of $\Delta N_x(\lambda)$ from the wavelength dependence of $\Delta N_y(\lambda)$ as shown in Fig. 4 by the dashed line. The chromatic-dispersion difference is negative and it decreases with wavelength, which causes, as illustrated in Fig. 5, the chromatic dispersion $D_x(\lambda)$ to be lower than $D_y(\lambda)$ and with greater separation at longer wavelengths.

In Fig. 5 is also shown the material dispersion of pure silica glass. The chromatic dispersion for the polarization modes of the fibre is higher than that for the pure silica glass. The difference between these dispersions can be attributed to the waveguide dispersion that is higher for longer wavelengths than for shorter ones. This behavior is expected due to the well-known fact that the contribution from waveguide dispersion increases with wavelength. Physically, this is because the mode is well confined to the core for short wavelengths, and the light therefore primarily interacts with the bulk material; as the mode size increases with wavelength, the light will increase its interaction with the surrounding air holes of the fibre. The ZDWs λ^x_{ZDW} and λ^y_{ZDW} for each polarization modes are 1065.7 nm and 1051.3 nm, respectively.

Next, the group modal birefringence dispersion was measured for the remaining HFs. Least-squares fits of $G(\lambda)$ according to Eq. (7) to the experimental data are shown for all HFs in Fig. 7 and Table 2 lists the corresponding parameters m and ξ. It is clearly seen from Fig. 7 that the smaller the geometrical parameters of the HFs, the greater the absolute value of the group modal birefringence and the quicker its change with wavelength. Table 2 shows that parameter ξ decreases and parameter m increases with the enlargement of the geometrical parameters of the HFs.

Similarly, Fig. 8 shows the chromatic-dispersion difference $D_p(\lambda)$ as a function of wavelength λ evaluated by using Eq. (9) for all HFs. The chromatic-dispersion differences are negative and they decrease with wavelength. The smaller the geometrical parameters of the HFs, the greater the absolute value of the chromatic-dispersion difference and the quicker its change with wavelength. The measured chromatic dispersions $D_x(\lambda)$ and $D_y(\lambda)$ are depicted in Fig. 9 in the vicinity of the ZDWs. It is clearly seen that the smaller the geometrical parameters of the HFs, the shorter the ZDWs λ^x_{ZDW} and λ^y_{ZDW} (see also Table 2). It should be noted that the most suitable fibre from the point of view of supercontinuum generation is HF 2, for which the ZDW $\lambda^x_{\mathrm{ZDW}} = 1065.7$ nm is close to a 1064 nm of a pump Nd:YAG Q-switched laser.

5 Conclusions

In this paper we presented a spectral interferometric technique for measuring the chromatic dispersion and the ZDW of polarization modes supported by short-length HFs. The technique, which is substantially improved in comparison with our previous technique [11], utilizes a broad-band supercontinuum source and a dispersion balanced MZI. The MZI with a fibre in the test arm is used to measure the wavelength dependence of the differential group effective index, or equivalently the chromatic dispersion of polarization modes supported by the fibre. A five-term power series fit is applied to the measured

data to obtain the chromatic dispersion over a broad spectral range (500–1600 nm). We measured by this technique the chromatic dispersion of polarization modes in four pure silica highly birefringent HFs and revealed the dependence of the position of the ZDW on the geometrical parameters of the HF. We have revealed that the ZDW for the x-polarization mode of one of the HFs is close to a wavelength of 1064 nm, which makes it a very good candidate for future construction of a supercontinuum source pumped by a Nd:YAG microchip laser. Moreover, our new approach utilizing the supercontinuum source instead of a halogen lamp makes a broad spectral range measurement of chromatic dispersion of polarization modes in short-length optical fibres accurate and less time consuming.

Acknowledgements The research was partially supported by the Grant Agency of the Czech Republic through grant P102/11/0675, and by the regional grant CZ.1.05/2.1.00/01.0040.

References

[1] Cohen LG. Comparison of single-mode fiber dispersion measurement techniques. J Lightwave Technol 1985;3:958–966.

[2] Costa B, Mazzoni D, Puleo M, Vezzoni E. Phase shift technique for the measurement of chromatic dispersion in optical fibers using LED's. IEEE J Quantum Electron 1982;118:1509–15.

[3] Diddams S, Diels JC. Dispersion measurements with white-light interferometry. J Opt Soc Amer B 1995;13:1120–8.

[4] Tateda M, Shibata N, Seikai S. Interferometric method for chromatic dispersion measurement in a single-mode optical fiber. IEEE J Quantum Electron 1981;17:404–7.

[5] Merritt P, Tatam RP, Jackson DA. Interferometric chromatic dispersion measurements on short lengths of monomode optical fiber. J Lightwave Technol 1989;7:703-16.

[6] Ye Q, Xu C, Liu X, Knox WH, Yan MF, Windeler RS, Eggleton B. Dispersion measurement of tapered air-silica microstructure fiber by white-light interferometry. Appl Opt 2002;41:4467–70.

[7] Lu P, Ding H, Mihailov SJ. Direct measurement of the zero-dispersion wavelength of tapered fibres using broadband-light interferometry. Meas Sci Technol 2005;16:1631–6.

[8] Galle MA, Mohammed W, Qian L, Smith PWE. Single-arm three-wave interferometer for measuring dispersion of short lengths of fiber. Opt Express 2007;16:16896–908.

[9] Hlubina P, Szpulak M, Ciprian D, Martynkien T, Urbańczyk, W. Measurement of the group dispersion of the fundamental mode of holey fiber by white-light spectral interferometry. Opt Express 2007;15:11073–81.

[10] Zhang T, Yang Z, Zhao W, Wang Y, Fang P, Li C: Dispersion measurement of Yb-doped fiber by a spectral interferometric technique. Chin Opt Lett 2008;8:262–5.

[11] Hlubina P, Ciprian D, Kadulová M. Measurement of chromatic dispersion of polarization modes in optical fibres using white-light spectral interferometry. Meas Sci Technol 2010;21:045302.

[12] Hlubina P, Kadulová M, Ciprian D. Spectral interferometry-based chromatic dispersion measurement of fibre including the zero-dispersion wavelength. J Eur Opt Soc Rapid Publ 2012;7:12017.

[13] Lee JY, Kim DY. Versatile chromatic dispersion measurement of a single mode fiber using spectral white light interferometry. Opt Express 2006;14:11608–14.

[14] Galle MA, Saini SS, Mohammed WS, Qian L. Chromatic dispersion measurements using a virtually referenced interferometer. Opt Lett 2012;37:1598–1600.

[15] Ouzounov D, Homoelle D, Zipfel W, Webb WW, Gaeta AL, West JA, Fajardo JC, Koch KW. Dispersion measurements of microstructure fibers using femtosecond laser pulses. Opt Commun 2001;192:219–23.

[16] Labonté L, Roy P, Pagnoux F, Louradour F, Restoin C, Mélin G, Burov E. Experimental and numerical analysis of the chromatic dispersion dependence upon the actual profile of small core microstructured fibres. J Opt A: Pure Appl Opt 2006;8:933–8.

[17] Dudley JM, Genty G, Coen S. Supercontinuum generation in photonic crystal fiber. Rev Mod Phys 2006;78:1135–85.

[18] Wadsworth WJ, Joly N, Knight JC, Birks TA, Biancalana F, Russell PStJ. Supercontinuum and four-wave mixing with Q-switched pulses in endlessly single-mode photonic crystal fibres. Opt Express 2004;12:299–309.

[19] Lehtonen M, Genty G, Ludvigsen H, Kaivola M. Supercontinuum generation in a highly birefringent microstructured fiber. Appl Phys Lett 2003;82:2197–9.

[20] Xiong C, Wadsworth WJ. Polarized supercontinuum in birefringent photonic crystal fibre pumped at 1064 nm and application to tuneable visible/UV generation". Opt Express 2008;16:2438–45.

[21] Ortigosa-Blanch A, Knight JC, Wadsworth WJ, Arriaga J, Mangan BJ, Birks TA, Russell PStJ. Highly biregringent photonic crystal fibers. Opt Lett 2000;25:1325–7.

[22] Hlubina P, Ciprian D, Kadulová M. Wide spectral range measurement of modal birefringence in polarization-maintaining fibres. Meas Sci Technol 2009;20:025301.

Table 1
Cladding diameter Φ, pitch Λ, diameter d of small holes, diameter D of large holes and length z of measured HFs.

FUT-HF	Φ (μm)	Λ (μm)	d (μm)	D (μm)	z (mm)
HF 1	154	4.25	1.53	4.25	77.640
HF 2	126	3.57	1.36	3.57	78.800
HF 3	103	3.40	1.19	3.40	78.910
HF 4	85	2.42	0.85	2.55	73.400

Table 2
Measured parameters m, ξ and λ_{ZDW} of HFs.

FUT-HF	m	ξ (nm^{-m})	λ^x_{ZDW} (nm)	λ^y_{ZDW} (nm)
HF 1	2.508	$4.852 \cdot 10^{-12}$	1095.1	1081.7
HF 2	2.274	$3.957 \cdot 10^{-11}$	1065.7	1051.3
HF 3	2.090	$3.091 \cdot 10^{-10}$	1011.0	991.9
HF 4	2.080	$4.055 \cdot 10^{-10}$	963.0	943.4

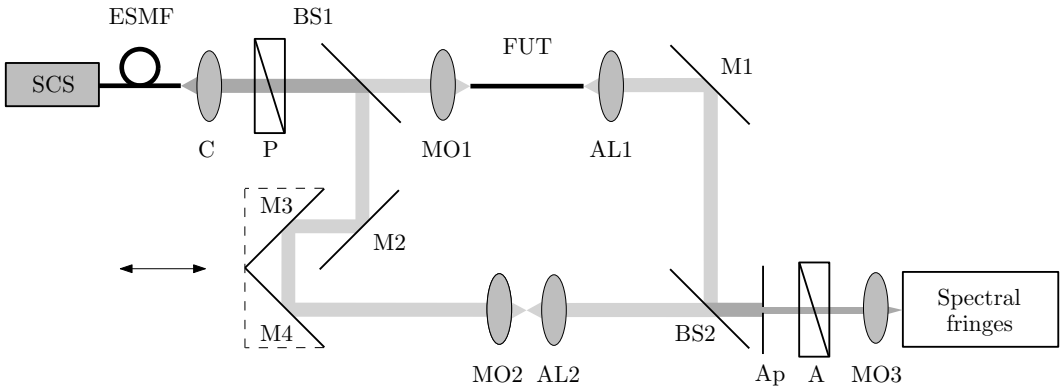

Fig. 1. Experimental set-up with a dispersion balanced Mach-Zehnder interferometer to measure the chromatic dispersion of polarization modes in a birefringent fibre (SCS: supercontinuum source, ESMF: endlessly single-mode fibre, C: collimator, P: polarizer, BS: beam splitter, MO: microscope objective, FUT: fibre under test, AL: achromatic lens, Ap: aperture, A: analyzer).

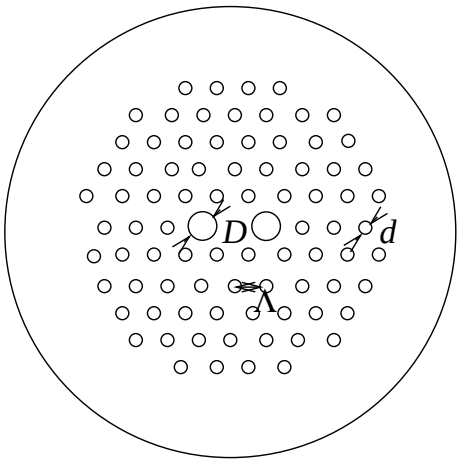

Fig. 2. Geometry of the investigated HFs.

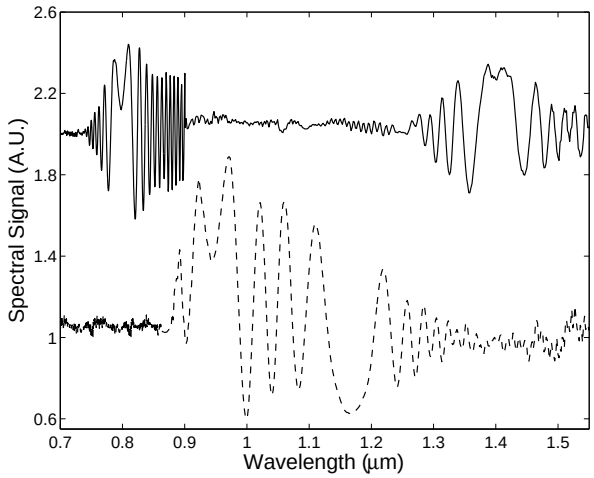

Fig. 3. Examples of two spectral signals recorded for HF 2 and corresponding to two different path length differences $\Delta L_1 = -640$ μm (solid line) and $\Delta L_1 = -820$ μm (dashed line) adjusted in the MZI.

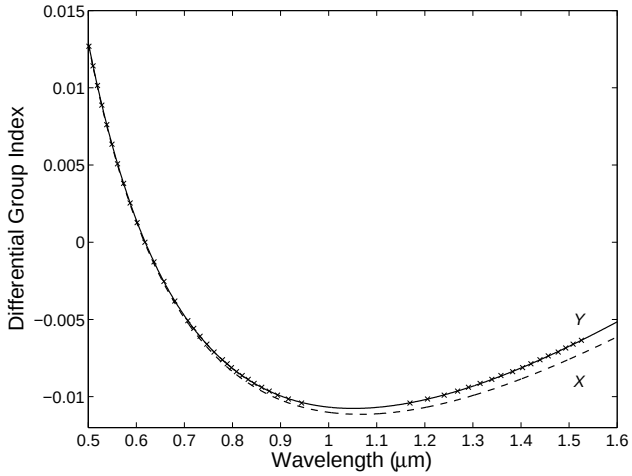

Fig. 4. Differential group index of two polarization modes in HF 2 as a function of wavelength. Measured values are the crosses and the solid line is a fit.

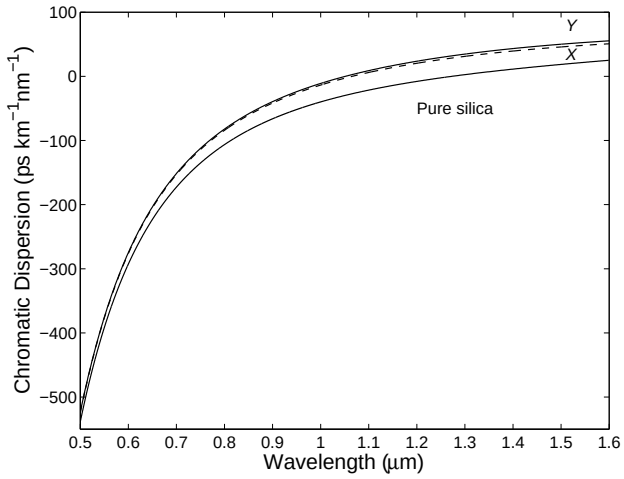

Fig. 5. Chromatic dispersion of two polarization modes in HF 2 and in pure silica as a function of wavelength.

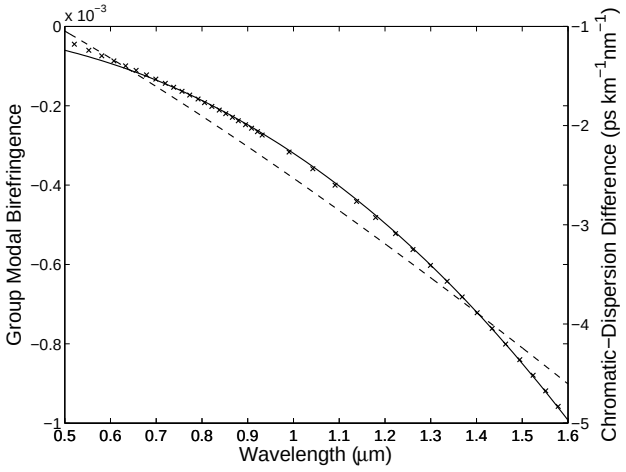

Fig. 6. Measured group modal birefringence (crosses) in HF 2 with a fit (solid line) and the chromatic-dispersion difference as a function of wavelength (dashed line).

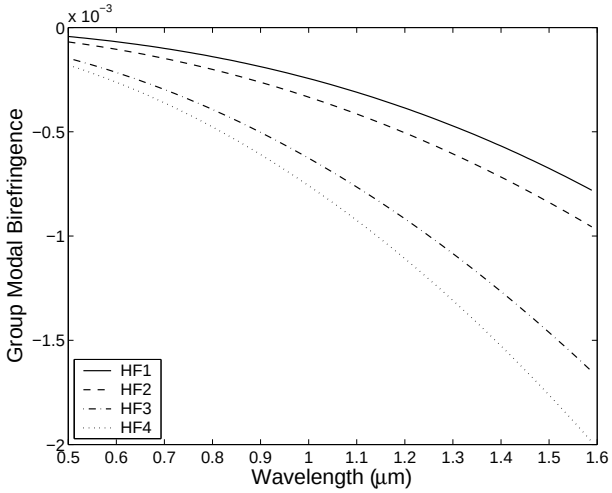

Fig. 7. Group modal birefringence in HFs as a function of wavelength.

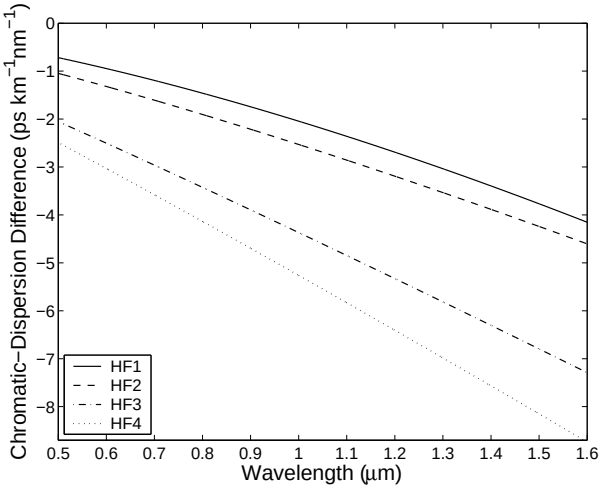

Fig. 8. Chromatic-dispersion difference in HFs as a function of wavelength.

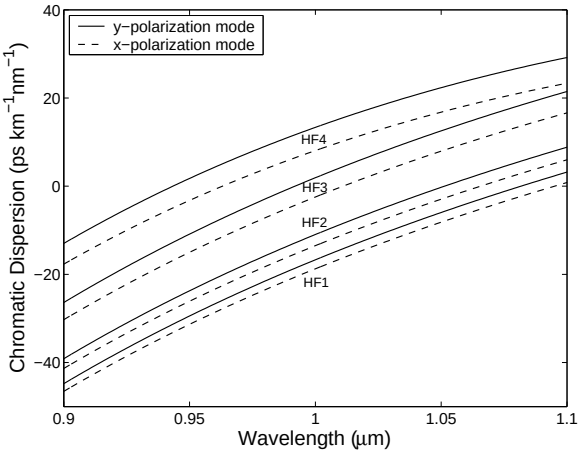

Fig. 9. Chromatic dispersion of the polarization modes in HFs as a function of wavelength (near the ZDWs).